Coronal Mass Ejections: Masses, Dynamics and Shock Kinematics

A dissertation submitted to the University of Dublin
for the degree of *Philosophiæ Doctor (PhD)*

Eoin P. Carley
Trinity College Dublin, December 2013

SCHOOL OF PHYSICS
UNIVERSITY OF DUBLIN
TRINITY COLLEGE

Declaration

I declare that this thesis has not been submitted as an exercise for a degree at this or any other university and it is entirely my own work.

I agree to deposit this thesis in the University's open access institutional repository or allow the library to do so on my behalf, subject to Irish Copyright Legislation and Trinity College Library conditions of use and acknowledgement.

Name: Eoin Carley

Signature: .... **Date:** ....

Summary

Coronal mass ejections (CMEs) are large-scale eruptions of magnetized plasma from the low solar atmosphere into interplanetary space. With energies of up to 10^{26} J, they are the most energetic eruptive phenomena in the solar system and are also the driver of plasma shocks from the corona into the heliosphere. Despite many years of study, the nature of the forces governing their eruption, and the kinematical behavior of the resulting shock, remain poorly understood. This thesis will presents the first accurate calculation of the magnitude of the total force on a CME. I will also show a previously unseen plasma shock behavior that sheds new light into the kinematical nature of CME-driven shocks in the corona.

In the past, measurement of the forces governing the propagation of CMEs have been hindered by highly uncertain estimates of the total mass of the ejection. The primary source of uncertainty is the unknown position and geometry of the CME, leading to an erroneous treatment of the Thomson scattering equations which are used to estimate the mass. Geometrical uncertainty on the CMEs position and size has primarily been due to observations of the eruption from a single vantage point. However, with the launch of the STEREO spacecraft, the two viewpoints can be exploited to derive the CMEs position and size, ultimately resulting in mass uncertainty that is both reliably quantified and much reduced. These much better estimates for the mass can then be combined with kinematical results that are also more reliable and hence lead to the first reliable quantification of the total force acting on the CME.

This thesis will present the method by which mass values derived from the STEREO coronagraphs, and the uncertainties reliably quantified. Combining this with a previous kinematical analysis, the mechanical energies and total force on the CME is derived. Using the magnetohydrodynamical equation of motion, the relative sizes of the forces at each stage in the CME propagation are estimated, revealing the Lorentz force is the largest source of CME acceleration early in its propagation. This analysis also leads to a reliable observational estimate of size of this Lorentz force.

CMEs often erupt at speeds in excess of the local MHD wave speeds in the corona. Traveling in excess of Mach 1, they often drive shocks which can have a variety of manifestations, from radio bursts to the propagation of bright pulse seen in extreme ultraviolet (EUV) images. Despite these myriad shock phenomena being observed for decades, the relationship between them remains unknown. Chapters X and Y of this thesis, will describe the construction of instrumentation to observe high time sampling spectroscopy of these radio bursts. These observations are combined with high cadence radio and EUV images to reveal the presence of a shock driven by the expansion of the CME flank that resulted in both the EUV pulse and radio burst. Furthermore, the radio spectra evidence for particle acceleration at this shock is presented, revealing the shock was capable of producing a bursty acceleration of near-relativistic electrons. This previously unseen behavior sheds new light on the physics governing radio burst generation and the relationship to CMEs and EUV pulses.

For my parents.

Acknowledgements

Some sincere acknowledgements...

List of Publications

1. **Carley, E. P.**, MacAteer, R. T. J., & Gallagher, P. T.
   "Coronal Mass Ejection Masses, Energies, and Force Estimates Using *STEREO*",
   The Astrophysical Journal, Volume 752, Issue 1, article id. 36, 8 pp. (2012).

2. Zucca, P., **Carley, E. P.**, McCauley, J., Gallagher, P. T. ,Monstein, C., &
   MacAteer, R. T. J.,
   "Observations of Low Frequency Solar Radio Bursts from the Rosse Solar-
   Terrestrial Observatory",
   Solar Physics, Volume 280, Issue 2, pp.591-602. (2012).

3. **Carley, E. P.**, Long, D. M., & Gallagher, P. T.
   "Shock Acceleration of Energetic Particles in the Solar Atmosphere",
   Some Journal, Volume X, Issue Y, article id. (2013)

4. Zucca, P., **Carley, E. P.**, Bloomfield, S. D., & Gallagher, P. T.
   "Density and Alfvén....",
   Some Journal, Volume X, Issue Y, article id. (2013)

5. Bloomfield, S. D., **Carley, E. P.**,
   "A Comprehensive Overview of the 2011 June 7 Solar Storm",
   Astronomy & Astrophysics, Volume X, Issue Y, article id. (2013)

Contents

List of Figures

List of Tables

1

Introduction

The Sun has long been the focus of humanity's curiosity. Throughout history it has been the harbinger of new religions, philosophies, and sciences. It has changed our understanding of our place in the Universe and allowed us to push forward the frontiers of stellar astronomy. Although our understanding of the Sun is nowadays more advanced, the curiosity we hold for it has not changed since the very early humans. Now, we understand the Sun is a star similar to any other in its class, currently going through a relatively unchanging 11 year cycle of activity that is extremely rich in physical complexity. The study of such complex phenomena has yielded immeasurable advances in many areas of physics such as spectroscopy, plasma physics, magnetohydrodynamics (MHD), particle physics, to name but a few. Although some of these sciences have grown over decades (or even centuries) they are still incomplete. I hope this theses, in some small way, will contribute to the continuing growth of these sciences and to the understanding of our nearest star.

1.1 The Sun

The Sun is our nearest star, located 1.49×10^6 km from Earth at the centre of our solar system. Located on the main sequence of the Hetzpring-Russel (HR) diagram, it has a spectral class of G2V, with a luminosity of $L_\odot = (3.84 \pm 0.04) \times 10^{26}$ W, mass of $M_\odot = (1.989 \pm 0.0003) \times 10^{30}$ kg and radius of $R_\odot = (6.959 \pm 0.007) \times 10^8$ m (Foukal, 2004). It was born approximately 4.6×10^9 years ago when a giant molecular cloud underwent gravitational collapse and began hydrogen nuclear fusion at its centre (reference). The energy produced from this fusion resulted in enough pressure to counteract gravitational contraction and bring about a hydrostatic equilibrium, allowing the young star to reach a stability that is sustained today. It is estimated the Sun will maintain this stability for another 5 billion years, at which point, it will move off the main sequence and into a red giant phase. During this later part of its life, it will grow in size to 100 times its current radius and begin nuclear burning of heavier elements such as carbon and oxygen. Once carbon burning in the core has ceased it can no longer sustain nuclear fusion of heavier elements, resulting in a gravitational instability that will eventually lead to a stellar nova. This nova will result in the loss of the outer envelopes and ultimately the Sun's death, leaving behind a compact and dense white-dwarf.

Until such time, the Sun will remain on the main sequence in a regular state of hydrogen fusion in its core. The energy released during this process is the ultimate source of light and all energetic activity that we observe from Earth and beyond. Before we can understand how this energy manifests in the solar atmosphere as a variety of energetic phenomena, it is important to understand how the energy is generated and transported through its interior and finally released into its atmosphere and interplanetary space.

1.1.1 Solar Interior

The theoretical development on how the solar interior is structured and how it behaves has been through what is known as the 'standard solar model' or SSM. The SSM is a grouping of theories that described how the Sun was formed, how it maintains its stability, how it generates energy, and how this energy is transported

through its interior and released at the surface. Much of the major developments of this theory have been in the 20th century, due mainly to the pioneering experiments in solar neutrino physics and helioseismsology. Hence, the development of the SSM has mainly been through a refinement of the theory based on these observational fields. Although the SSM has increased in sophistication, its four main aspects remain the most general framework for describing the behavior of the solar interior.

The SSM firstly states that the Sun was born from the gravitational collapse of a primordial gas of hydrogen, helium, and traces of other heavy elements. Secondly, it maintains its structural stability via a hydrostatic equilibrium such that the gravitational force is balanced by a pressure gradient ($\nabla P = -\rho g$) at each radial distance inside the star. The third main aspect of the SSM involves the source of the Sun's energy. Much of the early ideas proposed during the 19th century involved some form of chemical reaction or energy released during a slow gravitational contraction. However, during the first half of the 20th century the theory that the Sun is at least as old as the Earth began to come into focus. The idea of the Sun being more than 4.5 billion years old prompted the question of what energy source could sustain the Sun's luminosity for such a length of time. It was soon realised that thermonuclear fusion must be the source of such energy, and, as a result, it should be possible to observe the neutrino products of this fusion. Hence, starting in the 1950s a number of pioneering neutrino physics experiments were developed in an attempt to detect solar-generated neutrinos at Earth. These pioneering experiments, as well as there more sophisticated counterparts today, confirm much of the theories on solar core energy generation.

From the 1950s onwards there has been a confirmed detection of neutrinos generated in a hydrogen fusion process, namely the proton-proton or 'pp'-chain, in the solar core. In this process, four protons are fused to form a helium nucleus. This can occur in a variety of ways, but at the Sun's core temperature of 15 MK, the dominant reaction is the pp 1 chain given by

$$
{}^{1}_{1}\mathrm{H} + {}^{1}_{1}\mathrm{H} \rightarrow {}^{2}_{1}\mathrm{H} + e^{+} + \nu_{e} \tag{1.1}
$$

$$
{}^{2}_{1}\mathrm{H} + {}^{1}_{1}\mathrm{H} \rightarrow {}^{3}_{2}\mathrm{He} + \gamma \tag{1.2}
$$

$$\ce{^3_2He} + \ce{^3_2He} \rightarrow \ce{^4_2He} + 2\ce{^1_1H} \tag{1.3}$$

where $\ce{^1_1H}$ is a hydrogen nucelus, $\ce{^2_1H}$ is deuterium, $\ce{^3_2He}$ is tritium, $\ce{^4_2He}$ is helium, e^+ is a positron, ν_e is an electron neutrino, and γ is a gamma ray photon. Reactions (1.1) and (1.2) must happen twice for (1.3) to occur. Taking this into account, the entire process may be summarised as

$$4\ce{^1_1H} \rightarrow \ce{^4_2He} + 2e^+ + 2\nu_e + 2\gamma \tag{1.4}$$
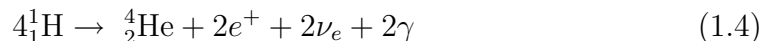
liberating 4.2×10^{-12}J of energy, with $\sim 2.4\%$ of the energy carried away by the neutrinos. This particular form of the pp-chain (pp 1) occurs in 86% of the cases (Turck-Chièze & Couvidat, 2011). However, there are other reactions capable of producing He from H catagorized into pp II, pp III etc, which each involve production of $\ce{^7_4Be}$ and $\ce{^8_5B}$. The initial neutrino detections at Earth were the result of the pp III reaction which involves the creation of $\ce{^8_5B}$, followed by a decay to $\ce{^8_4Be}$, a positron, and an electron neutrino (Davis *et al.*, 1968). These early detections and the results of more recent experiments such as the SuperKamiokande (Fukuda *et al.*, 1998) show that the expected neutrino flux given by the standard solar model is smaller than the observed. This deficit in in neutrino flux observations became the famed 'solar neutrino problem' during the 1970s. One of the proposed explanations for the process was via an oscillation of the neutrino amongst three sets of 'flavors' i.e., the neutrino can be either an electron ν_e, muon ν_μ, or tau ν_τ neutrino. With the original detectors only being able to detect the ν_e, this would result in a flux deficit (non-detection of ν_μ and ν_τ). This oscillation amongst three flavors was given the name the 'MSW effect' after Mikheev & Smirnov (1986) and Wolfenstein (1978), and later confirmed experimentally by the SuperKamionkande experiment.

The neutrino experiments together with the standard solar model SSM provide much of what we know about the solar energy generation and the solar core. They imply a temperature of 15.6×10^6K and density of $1.48 \times 10^5 \, \mathrm{kg\,m^{-3}}$ at solar centre, and also confirm the existence of a variety of pp reactions (pp 1 to pp IV), and some level of Carbon-Nitrogen-Oxygen (CNO) fusion process. These fusion processes occur over $0.0 - 0.25 \, R_\odot$ (Figure 1.1), which defines the solar core. Outside the core the temperature drops to a value such that fusion ceases.

While thermonuclear fusion is the third aspect of the SSM involves the generation of solar energy, the fourth aspect involves exactly what happens to this energy once it is generated i.e., it describes an energy transport mechanism.

Beyond $0.25\,R_\odot$ the temperature drops to 8 MK, such that fusion stops but only free protons and electrons exist. In this environment, the photons continuously scatter off free particles, undergoing a random walk toward the surface over a distance of $0.25 - 0.7\,R_\odot$. This region is known as the radiative zone and has densities of $2 \times 10^4 - 2 \times 10^2\,\mathrm{kg\,m^{-3}}$, resulting in a small photon mean free path (mfp) of $9.0 \times 10^{-4}\,\mathrm{m}$. The photons proceed towards the solar surface over a very long time scale, taking on the order of 10^5 years to traverse this region (Mitalas & Sills, 1992). If radiative energy transport occurs, it will result in the following temperature gradient

$$\frac{dT}{dr} = -\frac{3}{16\sigma}\frac{\kappa\rho}{T^3}F_{rad} \tag{1.5}$$

where σ is the Stefan-Boltzman constant, κ is the mass extinction coefficient (opacity per unit mass), ρ is mass density, T is temperature, and F_{rad} is the outward radiative flux. This implies that for a particular outward flux, if the opacity increases, a steeper temperature gradient is required to maintain such a flux. At $0.7\,R_\odot$ the temperature drops to $0.5\,\mathrm{MK}$ allowing protons to capture electrons into a bound orbit. The existence of electrons in atomic orbit results in a dramatic increase in opacity of the plasma (Turck-Chièze & Couvidat, 2011) and hence the temperature gradient increases. The increased temperature gradient required to sustain the energy flow may lead to the onset of a convective instability beyond $0.7\,R_\odot$ toward the solar surface. This instability will occur if the temperature gradient in the star is steeper than the adiabatic temperature gradient

$$\left|\frac{dT}{dr}\right|_{star} > \left|\frac{dT}{dr}\right|_{adiabatic} \tag{1.6}$$

This is known as the Schwarzschild criterion, and it is fulfilled from $0.7 - 1\,R_\odot$ −a region known as the convection zone. The temperature and density drop as height increases and finally reaches T$\sim$6000 K and mass densities of $\rho \sim 1 \times 10^{-5}\,\mathrm{kg\,m^{-3}}$. Although no complete theoretical treatment of convection exists, mixing length theory and hydrodynamical modeling are used to determine how convection occurs in the solar interior.

Much of what we know about the depth, temperature, and density of the core, radiative, and convection zones come from a fine-tuning of the standard solar model, such that the model reproduces observations from neutrino and helioseismology experiments. In fact helioseismology alone can indicate great detail of the internal structure of the Sun. It has revealed that both the core and radiative zone rotate as a rigid body, while the convective zone undergoes differential rotation (REFERENCE), in much the same way as the solar surface does. Hence the boundary between the radiative and convective zones mark a region where the internal dynamics of the Sun change dramatically. This boundary is known as the tachocline, and it is this region that is of much relevance to the generation and cyclic evolution of the Sun's magnetic field.
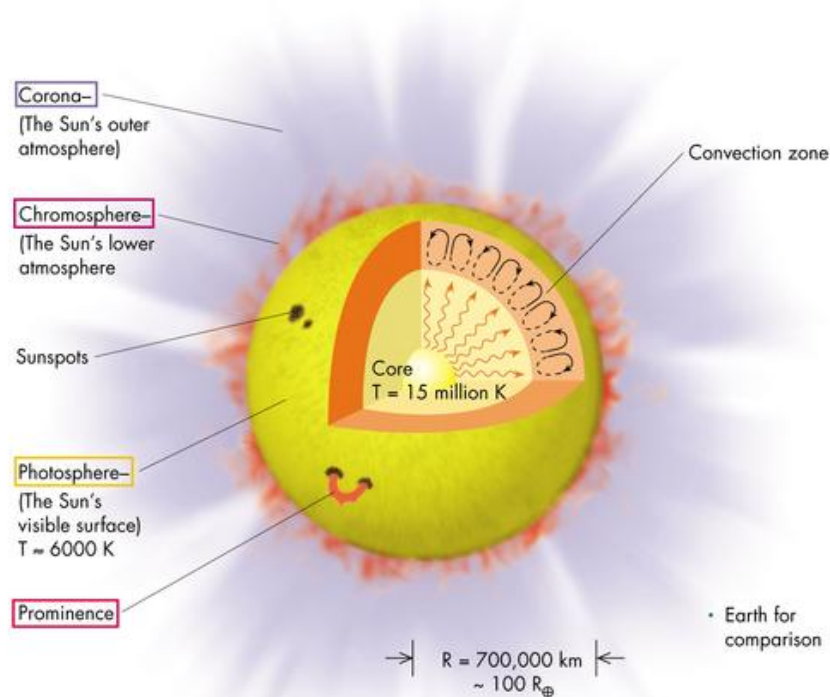
Figure 1.1: The internal structure of the Sun, including the core, radiative zone, and convective zone. Also shown is the structure of the its atmosphere, including the photosphere, chromosphere, and corona. The layers of the solar atmosphere are usually demarcated by temperature changes as height above the solar surface increases. The temperature ranges from ∼6000 K in the photosphere to above 1 MK in the corona.

1.1.2   Solar Dynamo and Magnetic Field

- Cellular pattern in photosphere is very different to the convective structure in deeper layers.
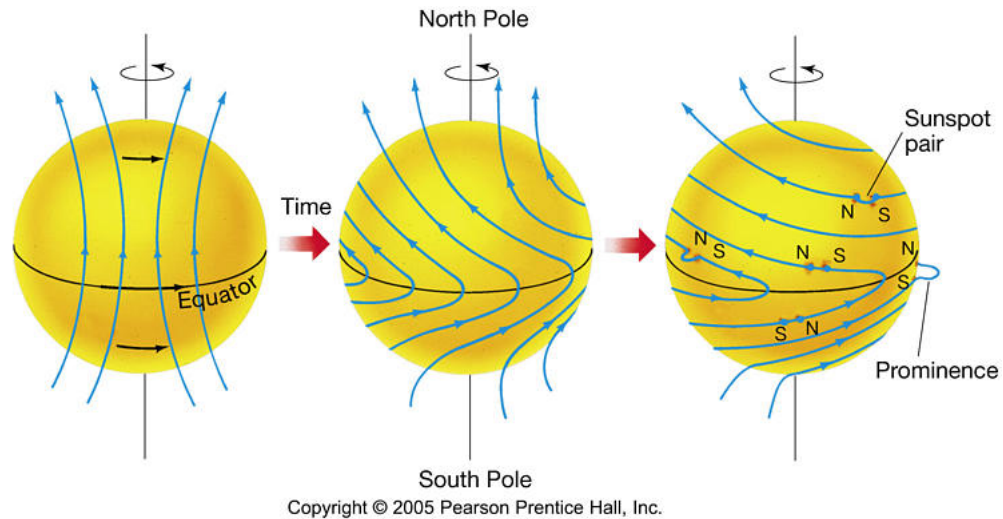
Figure 1.2: Differential rotation and flux freezing result in the poloidal dipolar magnetic field, generated by dynamo action, to be dragged around in a toroidal direction, an action known as the omega effect. Buoyancy of the field lines results in them rising and twisting, known as the alpha effect, eventually surfacing to become bipolar fields that extend far into the corona.

It is widely believed that the Sun's magnetic field is created by a dynamo action in a region between the radiative zone and the convection zone, known as the tachocline. Solar dynamo theory attempts to explain the observed 11 year magnetic activity cycle, where the the Sun's magnetic field starts as a poloidal dipolar structure and evolves to having a strong toroidal component, after which it returns to a poloidal field again. During these 11 years the Sun starts at minimum activity, reaches a maximum and returns to minimum again.

Babcock (1961) first explained this process by a mechanism involving differential rotation of the solar surface and interior. The equatorial rotation rate is faster than the rotation rate at higher latitudes. Because the magnetic field is frozen into the plasma, any flows in the solar interior will tend to drag the magnetic field along. By this effect, differential rotation tends to drag the field and

wrap it around the Sun in a toroidal direction, this is known as the omega effect, see Figure 1.2.

As the toroidal field builds up in the solar interior, sections of field lines build up in magnetic pressure resulting in a buoyancy of the field. The field slowly rises through the convection zone and eventually surfaces as a bipolar region that extends into the solar atmosphere. The presence of bipolar fields in the solar atmosphere and their slow build up over time to complex magnetic structures, known as active regions, ultimately leads to a variety of eruptive phenomena.

1.1.3 Solar Atmosphere

1.1.3.1 Photosphere

- Appearance, Granules, Sunspots.

- Black Body Curve. Franhofer lines, H-alpha line, CaII H & K, H$^-$ alines, Sodium D lines.

- Temperature, Density, Opacity.

- Magnetic field strength

The most spectacular and energetic phenomena in our solar system have their origins in the solar atmosphere. This ever-changing and dynamic environment is a hotbed of activity giving rise to coronal mass ejections (CMEs), solar flares, and a host of plasma processes resulting in emission across the entire electromagnetic spectrum. To make sense of the phenomena we observe we must first have a basic understanding of solar atmospheric structure and the environment these processes take place in. Figure 1.1 is an illustration of the different layers of the solar interior, the solar surface and atmosphere. The visible surface of the Sun is known as the photosphere. It is demarcated where optical depth becomes unity for a wavelength of $5000\,\text{Å}$ or $\tau_{5000} = 1$. At such visible wavelengths, the electromagnetic spectrum is well represented by a blackbody of temperature T$\sim 6000\,\text{K}$. .

- Eddington Barbier, $\tau = \mu$, limb darkening.

8

- Effective temperature, $\tau = 2/3$, $T = 5800\,\mathrm{K}$

During periods of increased activity there may also be the presence of sunspots in the photosphere. These are dark features on the solar surface, see Figure 1.1, and are an indicator of concentrations of magnetic fields that are stronger than elsewhere in the quiet sun, as described above.

Photospheric abundances have been measured using emission line diagnostics were it is found that helium is the most abundant at 10.89^{1}, with the next most abundant elements being Carbon (8.58), Nitrogen (8.02), and Oxygen (8.8). All other elements have abundances that are 4 orders of magnitude or more less than hydrogen i.e., logarithmic abundances $\lesssim 7$ (Phillips *et al.*, 2008).

1.1.3.2   Chromosphere

- Appearance, Supergranular Network, Bright Points, Spicules, Filaments, Plage etc.

- Emission lines, H-alpha, CaII H & K.

- Temperature, Density, Opacity.

- Magnetic field strength.

At $\sim 500\,\mathrm{km}$ above the $\tau_{5000} = 1$ surface the temperature drops to a minimum of $\sim 4400\,\mathrm{K}$. Beyond this minimum the temperature begins to rise again, demarcating the beginning of the chromosphere. This layer of the atmosphere is generally accepted to extend to a height at which temperatures reach $20{,}000\,\mathrm{K}$, however temperatures as high as $\sim 1 \times 10^{5}\,\mathrm{K}$ are sometimes attributed to chromospheric heights, hence it is observable at ultraviolet (UV) wavelengths as well as visible.

---

[1] Abundances quoted relative to hydrogen on a logarithmic scale, $12.0 + log_{10}(A/A_H)$

1.1.3.3 Corona

- Appearance UV: Active regions, Coronal Loops, Holes.

- Emission lines, Mg, Ca, Fe, C, O etc.

- Appearance White-Light: Streamers, K, F, E corona

- Appearance Radio: thermal bremsstrahlung, free-free emissivity/opacity.

- Temperature, Density, Opacity, 'coronal heating problem'.

At a height of approximately 2,000 km the temperature begins to rise sharply while the number density of neutral hydrogen and electrons fall by several orders of magnitude. This rapid increase in temperature in such a short spatial extent (<100 km) is known as the transition region. It has a temperature on the order of 10^5 K and separates the relatively low temperature chromosphere and the high temperatures of > 1 MK in the corona. The reason for this rapid increase in temperature is still a hotly debated subject and a coronal heating mechanism remains largely unknown, this is known as the 'coronal heating problem'.

Element abundances in the corona show there is a similar composition to the photospheric abundances, with He, C, N, and O having the same ratios relative to H in the corona as that in the photosphere. The only difference is an enhancement in the abundance of low First Ionization Potential (< 10 eV) elements in the corona relative to the photosphere. For example, elements such as Na, Mg, Al, Si, Ca, Ni, and Fe can be up to three times more abundant in the corona (Feldman & Widing, 2003). The reason for the enhancement of low FIP elements in the corona is still unknown, however several models have suggested ion-neutral separation in the chromosphere by diffusion across magnetic fields, followed by transport of these ions into the corona may be viable mechanism (Geiss, 1985).

1.1.4 Solar Wind

- Parker's solution

- Parker Spiral

- Fast solar wind, Alfvén wave driver

- Mass loss rates (later compare CME mass loss)

1.2 Coronal Mass Ejections and Coronal Shocks

1.2.1 CMEs

- Appearance, white-light Illing, Hundhausen, Vourlidas

- Kinematics, velocity, acceleration

- Dynamics, masses, energies, forces

- Observations at other wavelengths, EUV, radio, SXR.

1.2.2 CMEs and Shocks

- Radio bursts, Type II, Type III

- Radio imaging of shocks

- Relationship to EUV waves, Moreton waves

1.2.3 Open Questions

2

Coronal Mass Ejection and Plasma Shock Theory

2.1 Plasma Physics and Magnetohydrodynamics

2.1.1 Maxwell's Equations

2.1.2 Plasma Physics and Boltzmann Equation

2.1.3 Magnetohydrodynamics

2.1.4 Magnetic Reconnection

2.1.5 MHD Rankine-Hugoniot Equations

2.1.6 Bow Shocks

2.2 Coronal Mass Ejections

2.2.1 Catastrophe Model

2.2.2 Magnetic Breakout Model

2.2.3 Toroidal Instability

2.2.4 Drag Models

2.3 Coronal Shocks

2.3.1 Shock Particle Acceleration

2.3.2 Wave-Particle Interaction

2.3.3 Electromagnetic Radiation in Plasma Shocks

3

Observation and Instrumentation

3.1 Thompson Scattering Theory

3.1.1 The van de Hulst Coefficients

3.1.2 Thomson Scattering in the Corona

3.1.3 White-light observations of CMEs

3.2 Conornagraphs

3.2.1 SOHO LASCO

3.2.2 STEREO CORs

3.3 Radio Spectrometers and Radioheliographs

3.3.1 RSTO Callisto

3.3.2 STEREO WAVES

3.3.3 Nancay Decametric Array

3.3.4 Nancay Radioheliograph

3.4 EUV imaging

3.4.1 SDO AIA

4

Coronal Mass Ejection Masses, Energetics, and Dynamics

4.1 Masses

4.1.1 Evaluation of Uncertainties

4.1.2 Masses

4.2 Energies and Dynamics

4.2.1 Mechanical Energy

4.2.2 Forces acting on CMEs

5

Coronal Mass Ejection Masses, Shocks, and Particle Acceleration

5.1 Radio Bursts

5.1.1 Type II, Type III, and Herringbones

5.2 EUV Wave and Radio Source

5.2.1 Relationship with Radio Spectra

5.3 Role of the CME

5.3.1 CME Bow Shock

5.3.2 Relationship Between CME, CBF, and Radio bursts

A A Nice Appendix

This is where the appendix would go...

References

BABCOCK, H.W. (1961). The Topology of the Sun's Magnetic Field and the 22-YEAR Cycle. *Astrophysical Journal*, **133**, 572. (Cited on page 7.)

DAVIS, R., HARMER, D.S. & HOFFMAN, K.C. (1968). Search for Neutrinos from the Sun. *Physical Review Letters*, **20**, 1205–1209. (Cited on page 4.)

FELDMAN, U. & WIDING, K.G. (2003). Elemental Abundances in the Solar Upper Atmosphere Derived by Spectroscopic Means. *Space Science Reviews*, **107**, 665–720. (Cited on page 10.)

FOUKAL, P.V. (2004). *Solar Astrophysics, 2nd, Revised Edition*. Wiley-VCH. (Cited on page 2.)

FUKUDA, Y., HAYAKAWA, T., ICHIHARA, E., INOUE, K., ISHIHARA, K., ISHINO, H., ITOW, Y., KAJITA, T., KAMEDA, J., KASUGA, S., KOBAYASHI, K., KOBAYASHI, Y., KOSHIO, Y., MARTENS, K., MIURA, M., NAKAHATA, M., NAKAYAMA, S., OKADA, A., OKETA, M., OKUMURA, K., OTA, M., SAKURAI, N., SHIOZAWA, M., SUZUKI, Y., TAKEUCHI, Y., TOTSUKA, Y., YAMADA, S., EARL, M., HABIG, A., HONG, J.T., KEARNS, E., KIM, S.B., MASUZAWA, M., MESSIER, M.D., SCHOLBERG, K., STONE, J.L., SULAK, L.R., WALTER, C.W., GOLDHABER, M., BARSZCZAK, T., GAJEWSKI, W., HALVERSON, P.G., HSU, J., KROPP, W.R., PRICE, L.R., REINES, F., SOBEL, H.W., VAGINS, M.R., GANEZER, K.S., KEIG, W.E., ELLSWORTH, R.W., TASAKA, S., FLANAGAN, J.W., KIBAYASHI, A., LEARNED, J.G., MATSUNO, S., STENGER, V., TAKEMORI, D., ISHII, T., KANZAKI, J., KOBAYASHI, T., NAKAMURA, K., NISHIKAWA, K., OYAMA, Y., SAKAI, A., SAKUDA, M., SASAKI, O., ECHIGO, S., KOHAMA, M., SUZUKI, A.T., HAINES, T.J., BLAUFUSS, E., SANFORD, R., SVOBODA, R., CHEN, M.L., CONNER, Z., GOODMAN, J.A., SULLIVAN, G.W., MORI, M., HILL, J., JUNG, C.K., MAUGER, C., MCGREW, C., SHARKEY, E., VIREN, B., YANAGISAWA, C., DOKI, W., ISHIZUKA, T., KITAGUCHI, Y., KOGA, H., MIYANO, K., OKAZAWA, H., SAJI, C., TAKAHATA, M., KUSANO, A., NAGASHIMA, Y., TAKITA, M., YAMAGUCHI, T., YOSHIDA, M., ETOH, M., FUJITA, K., HASEGAWA, A., HASEGAWA, T., HATAKEYAMA, S., IWAMOTO, T., KINEBUCHI, T., KOGA, M., MARUYAMA, T., OGAWA, H., SUZUKI, A., TSUSHIMA, F., KOSHIBA, M., NEMOTO, M., NISHIJIMA, K., FUTAGAMI, T., HAYATO, Y., KANAYA, Y., KANEYUKI, K., WATANABE, Y., KIELCZEWSKA, D., DOYLE, R., GEORGE, J., STACHYRA, A., WAI, L., WILKES, J. & YOUNG, K. (1998). Measurements of the Solar Neutrino Flux from Super-Kamiokande's First 300 Days. *Physical Review Letters*, **81**, 1158–1162. (Cited on page 4.)

GEISS, J. (1985). Diagnostics of corona by in-situ composition measurements at 1 AU. In E. Rolfe & B. Battrick, eds., *Future Missions in Solar, Heliospheric & Space Plasma Physics*, vol. 235 of *ESA Special Publication*, 37–50. (Cited on page 10.)

MIKHEEV, S.P. & SMIRNOV, A.I. (1986). Resonant amplification of neutrino oscillations in matter and solar-neutrino spectroscopy. *Nuovo Cimento C Geophysics Space Physics C*, **9**, 17–26. (Cited on page 4.)

MITALAS, R. & SILLS, K.R. (1992). On the photon diffusion time scale for the sun. *Astrophysical Journal*, **401**, 759. (Cited on page 5.)

PHILLIPS, K.J.H., FELDMAN, U. & LANDI, E. (2008). *Ultraviolet and X-ray Spectroscopy of the Solar Atmosphere*. Cambridge University Press. (Cited on page 9.)

TURCK-CHIÈZE, S. & COUVIDAT, S. (2011). Solar neutrinos, helioseismology and the solar internal dynamics. *Reports on Progress in Physics*, **74**, 086901. (Cited on pages 4 and 5.)

WOLFENSTEIN, L. (1978). Neutrino oscillations in matter. *Physical Review Letters*, **17**, 2369–2374. (Cited on page 4.)